

LETTER TO THE EDITOR

***MATR3* haploinsufficiency and early-onset neurodegeneration**

Michael Zech,^{1,2,†} Annette Seibt,^{3,†} Barbara Zumbaum,⁴ Dirk Klee,⁵ Thomas Meitinger,²
Juliane Winkelmann,^{1,2,6,7} Ertan Mayatpepek,³ Matias Wagner^{1,2} and Felix Distelmaier³

†These authors contributed equally to this work.

Author affiliations:

1 Institute of Neurogenomics, Helmholtz Zentrum München, Munich, Germany

2 Institute of Human Genetics, Technical University of Munich, Munich, Germany

3 Department of General Pediatrics, Neonatology and Pediatric Cardiology, University Children's Hospital, Medical Faculty, Heinrich-Heine-University, Düsseldorf, Germany

4 Sozialpädiatrisches Zentrum, St. Marien-Hospital Düren gGmbH, Hospitalstr. 44, 52353 Düren, Germany

5 Institute of Radiology, Department of Pediatric Radiology, Medical Faculty, Heinrich-Heine-University, Düsseldorf, Germany

6 Lehrstuhl für Neurogenetik, Technische Universität München, Munich, Germany

7 Munich Cluster for Systems Neurology, SyNergy, Munich, Germany

Correspondence to: Felix Distelmaier

Department of General Pediatrics, Heinrich-Heine-University, Moorenstr. 5, 40225 Düsseldorf, Germany

E-mail: felix.distelmaier@med.uni-duesseldorf.de

As recently reviewed in *Brain*, the knowledge about the monogenetic spectrum underlying familial amyotrophic lateral sclerosis (ALS) has grown substantially during the last years.¹ To date, 34 different genes have been linked to ALS, including *SOD1*, *TARDBP*, *FUS*, *TBK1*, *SETX*, *ALS2*, *DCTN1*, *VAPB*, *CHMP2B*, *ANG*, *FIG4*, *ATXN2*, *SPG11*, *VCP*, *OPTN*, *SIGMAR1*, *C9orf72*, *UBQLN2*, *SQSTM1*, *PFN1*, *HNRNPA1*, *ERBB4*, *MATR3*, *TUBA4A*, *CHCHD10*, *KIF5A*, *ANXA11*, *TIA1*, *NEK1*, *C21orf2*, *MOBP*, *SCFD1*, *CCNF*, and *GYLD*.^{1,2} Hypotheses regarding ALS development are numerous and comprise impaired mitochondrial function, dysregulation of protein degradation, disturbed axonal transport, alterations in autophagy, neuroinflammation, and aberrant regulation of cellular kinases. The shared end path of these pathomechanisms is selective motor neuron death leading to progressive muscle weakness,

bulbar palsy, and respiratory failure (clinical subtypes of ALS are reviewed by Masrori and Van Damme³). So far, no effective treatment is available for affected individuals.

In 2014, Johnson et al.⁴ identified variants in *MATR3* as a cause of familial ALS (ALS21, MIM # 606070). *MATR3* encodes nuclear protein matrin 3 (MATR3), which constitutes an important component of the nuclear matrix. MATR3 has DNA- and RNA-binding capacities and is involved in cell type-specific gene regulation, transcriptional regulation and DNA repair.⁵ Clinical features of *MATR3*-associated ALS include distal muscle weakness and bulbar signs, such as dysarthria and dysphagia. Some individuals show cognitive decline.⁶ No association of *MATR3* with pediatric diseases has been reported so far.

Interestingly, Park et al.⁷ described a 6-year-old boy with a homozygous truncating variant in *SOD1*, leading to early-onset neurodegeneration with developmental disability, tetraspasticity, and hyperekplexia-like features. The clinical phenotype was distinctly different compared to the classical manifestation in familial ALS patients with *SOD1* mutations. This demonstrates that genes linked to ALS may be associated with allelic conditions and thus a broader clinical spectrum than previously thought.

Comparable to the findings of Park et al.⁷, we here report on a child with a heterozygous *de novo* variant in *MATR3*, causing an early-onset disease phenotype with severe neurodegeneration that is distinctly different from previous reports on *MATR3*-associated disease.

The study was performed according to the declaration of Helsinki. Genetic and experimental procedures were undertaken after consent of the patient's parents was obtained. Written consent for the publication of photographs was obtained.

The boy was the second child of non-consanguineous parents with Romanian ancestry. A six-year-old sister and a one-year-old brother are healthy. He was born at term after an uneventful pregnancy (weight 3700 g, length 52 cm, head circumference according to the parents within normal range). After birth he showed muscular hypotonia and because of feeding difficulties a nasogastric tube was placed. First epileptic seizures occurred at the age of two months. Epilepsy was treated with valproate; however without achieving seizure freedom. Brain MRI at the age of four months revealed widening of outer and inner CSF spaces. Diagnostic work-up including screening for metabolic diseases (amino acids in plasma, organic acids in urine, transferrin electrophoresis, analysis of cerebrospinal fluid, purine and pyrimidine metabolites, analysis of very-long-chain fatty acid, etc.) was without specific findings. Genetic testing

including chromosome analysis, microarray analysis and genetic panel diagnostics (*ALDH7A1*, *CDKL5*, *FLOR1*, *KCNQ2*, *POLG*, *SCN1A*, *SLC2A1*, *STXBP1* and *ARX*) was normal.

At the current age of two years the boy shows severe microcephaly (head circumference <1st percentile, Z-score -5.72) and profound developmental disability (Figure 1 A-B). He is unable to move independently and shows profound muscular hypotonia. He shows a hypotonic-dystonic movement pattern, tendon reflexes are brisk. There is no speech development. Epilepsy is treated with levetiracetam und carbamazepine. Nevertheless, he is suffering from daily epileptic seizures (mostly short episodes with eye deviation and a duration of 20-30 seconds). EEG is pathological with high amplitude activity and predominantly left-sided epileptiform discharges. Brain MRI demonstrates supratentorial brain atrophy, delayed myelination and hypoplasia of the corpus callosum (Figure 1 C-D).

Whole-exome sequencing, performed on DNA from the child and both parents, failed to identify (likely) pathogenic variants in any genes previously associated with childhood-onset neurological disorders. The only suspicious finding was a *de-novo* transition (NM_018834.6: c.1306G>A; hg19: chr5:138653408G>A) in exon 7 of *MATR3*, predictably leading to the substitution of a highly conserved amino acid residue (p.Glu436Lys). The missense variant was absent from more than 280,000 control alleles in gnomAD and more than 40,000 alleles from in-house sequenced individuals with various clinical conditions. In silico evaluation predicted a deleterious effect of the variant (CADD score of 23.2; PolyPhen2 score of 0.99). Moreover, the site affected by the variant was expected to be intolerant against mutational changes and belongs to the 10% of most constraint coding regions of the genome (see also Supplementary Figure 1).⁸ Unlike ALS-linked *MATR3* missense variants predominantly affecting N- and C-terminal portions of the protein, c.1306G>A (p.Glu436Lys) mapped to the first of two central RNA-recognition motifs (RRM1; Figure 1). We were unable to identify any further *MATR3* *de-novo* changes in whole-exome sequencing data from more than 31,000 parent-offspring trios assessed for pediatric disorders, indicating that *de novo* missense variants are an extraordinarily rare mutational event.⁹ Notably, DECIPHER lists seven *de-novo* deletions encompassing *MATR3* in subjects with phenotypes overlapping that of the herein described child (developmental delay, muscular hypotonia, feeding difficulties, epilepsy), but there are no reported cases where *MATR3* alone has been deleted (<https://decipher.sanger.ac.uk/>).

To further investigate the functional consequences of the *MATR3* variant, we performed immunoblotting analysis of protein lysates derived from patient skin fibroblasts. In brief, cell culture was performed as described previously.¹⁰ Subcellular fractionation was performed using the NE-PER Nuclear and Cytoplasmic Extraction Kit (Thermo Scientific #78835) according to the manufacturer's protocol. Primary antibodies against *MATR3* (anti-rabbit; 1:1000; Proteintech #12202-2-AP), Lamin AC (anti-mouse, 1:5000; Thermo Scientific, SAB4200236) or GAPDH (anti-mouse, 1:4000; Thermo Scientific, AM4300) were used.

As depicted in Figure F-G we observed a significant reduction of about 50% of *MATR3* protein levels in nuclear fractions compared to healthy controls. This observation supports a disease-relevant role for c.1306G>A (p.Glu436Lys) given that metrics from gnomAD predict that dosage reduction of *MATR3* is not tolerated (probability of being loss-of-function intolerant score of 1.0; o/e = 0).

In addition to immunoblotting, we also performed *MATR3* immunofluorescence imaging. As depicted in Supplementary Figure 2, no obvious mislocalization or aggregation of *MATR3* was detectable in patient-derived cells.

The findings reported above suggest a disease-causing role of the *MATR3* variant identified in this study via a haploinsufficiency mechanism and a potential extension of *MATR3*-associated allelic conditions. Moreover, our results further support the notion that alterations in ALS-associated genes may have a crucial impact on neuronal viability and function. However, pediatric cases as now reported for *SOD1* and *MATR3* additionally point to the relevance of these genes for early neurodevelopment. This broadens our view on the physiological function of these genes. Moreover, it might have important implications for ALS treatment approaches that are currently under development. Several of these strategies aim for lowering levels of specific gene products since most mutations that have been identified in familial ALS are thought to be disease-causing by gain of function mechanisms.¹¹ However, the reports of Park et al.⁷ as well as the case illustrated here highlight the fact that both loss of function and gain of function mechanisms may have detrimental effects.

Data availability

The main data associated with this study are present in the article or Supplementary material. Additional raw data are available from the corresponding author, upon reasonable request.

Acknowledgements

First and foremost, all authors thank the family for participating in the study.

Funding

The study was supported by a grant of the German Research Foundation/Deutsche Forschungsgemeinschaft (DI 1731/2-2 to FD) and by a grant from the “Elterninitiative Kinderkrebsklinik e.V.” (Düsseldorf; #701900167).

Competing interests

The authors report no competing interests.

References

1. Guo W, Vandoorne T, Steyaert J, Staats KA, Van Den Bosch L. The multifaceted role of kinases in amyotrophic lateral sclerosis: genetic, pathological and therapeutic implications. *Brain*. 2020;143:1651-1673.
2. Dobson-Stone C, Hallupp M, Shahheydari H, et al. CYLD is a causative gene for frontotemporal dementia - amyotrophic lateral sclerosis. *Brain*. 2020;143:783-799.
3. Masrori P, Van Damme P. Amyotrophic lateral sclerosis: a clinical review. *Eur J Neurol*. 2020:1918-1929.
4. Johnson JO, Pioro EP, Boehringer A, et al. Mutations in the matrin 3 gene cause familial amyotrophic lateral sclerosis. *Nature Neurosci*. 2014;17: 664-666.
5. Malik AM, Barmada SJ. Matrin 3 in neuromuscular disease: physiology and pathophysiology. *JCI Insight*. 2021;6: e143948.
6. Marangi G, Lattante S, Doronzio PN, et al. Matrin 3 variants are frequent in Italian ALS patients. *Neurobiol Aging*. 2017;49:218.e1-218.e7.
7. Park JH, Elpers C, Reunert J, et al. SOD1 deficiency: a novel syndrome distinct from amyotrophic lateral sclerosis. *Brain*. 2019;142(8):2230-2237
8. Wiel L, Baakman C, Gilissen D, Veltman JA, Vriend G, Gilissen C. MetaDome: Pathogenicity analysis of genetic variants through aggregation of homologous human protein domains. *Hum Mutat*. 2019;40:1030-1038.
9. Kaplanis J, Samocha KE, Wiel L, et al. Evidence for 28 genetic disorders discovered by combining healthcare and research data. *Nature*. 2020;586:757-762

10. Wagner M, Skorobogatko Y, Pode-Shakked B, et al. Bi-allelic Variants in RALGAPA1 Cause Profound Neurodevelopmental Disability, Muscular Hypotonia, Infantile Spasms, and Feeding Abnormalities. *Am J Hum Genet.* 2020;106:246-255.
11. Kim G, Gautier O, Tassoni-Tsuchida E, Ma XR, Gitler AD. ALS Genetics: Gains, Losses, and Implications for Future Therapies. *Neuron.* 2020;108:822-842.

Figure legend:

Figure 1: A-B) Clinical photographs of the affected individual at the age of 2 years showing microcephaly. **C-D)** Brain MRI images at the age of 2 years (T2-weighted sequences, axial and sagittal views) demonstrating cerebral atrophy with widening of external and inner CSF spaces. Myelination is delayed and corpus callosum is severely hypoplastic (white arrow). **E)** Schematic domain representation of matrin 3. ALS-linked variants are shown in black and the variant identified herein is shown in red. Only those ALS-linked variants are depicted which are listed as “pathogenic” in ClinVar (<https://www.ncbi.nlm.nih.gov/clinvar/>). NLS, nuclear localization signal; RRM1, RNA-recognition motif 1; RRM2, RNA-recognition motif 2; ZF, zinc finger motifs. **F)** Representative immunoblot image depicting cytoplasmic and nuclear fractions of healthy controls (CT1-2 = age-matched male individuals, CT3 = age-matched female individual) and patient-derived (I#1) fibroblasts (the corresponding unmodified full-length blots can be found in the supplement). **G)** Quantitated density of immunoblot bands from four independent experiments. Average values are presented as the mean \pm SEM; ***p < 0.001 significantly different from controls. In patient-derived fibroblasts, nuclear MATR3 amounts are clearly reduced.

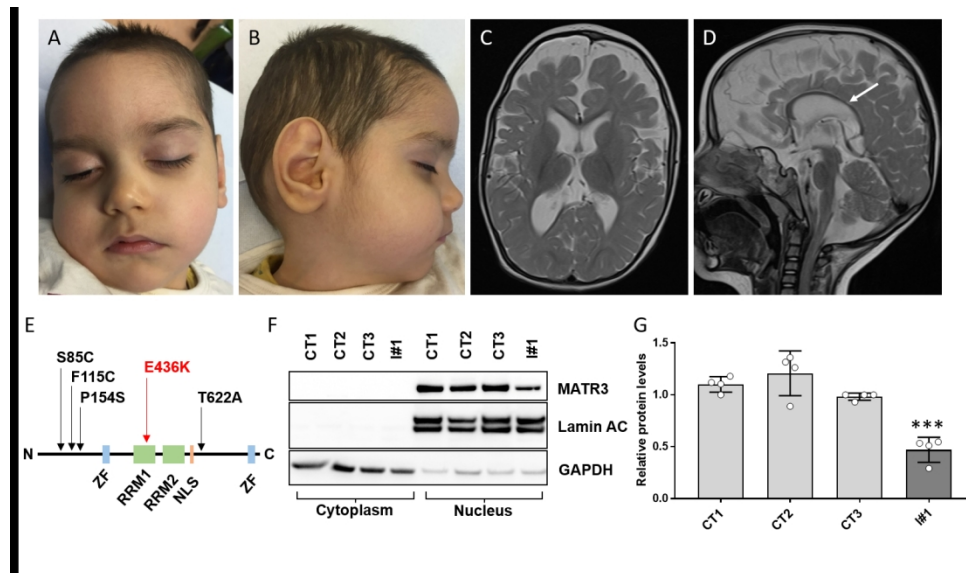


Figure 1: A-B) Clinical photographs of the affected individual at the age of 2 years showing microcephaly. C-D) Brain MRI images at the age of 2 years (T2-weighted sequences, axial and sagittal views) demonstrating cerebral atrophy with widening of external and inner CSF spaces. Myelination is delayed and corpus callosum is severely hypoplastic (white arrow). E) Schematic domain representation of matrin 3. ALS-linked variants are shown in black and the variant identified herein is shown in red. Only those ALS-linked variants are depicted which are listed as "pathogenic" in ClinVar (<https://www.ncbi.nlm.nih.gov/clinvar/>). NLS, nuclear localization signal; RRM1, RNA-recognition motif 1; RRM2, RNA-recognition motif 2; ZF, zinc finger motifs. F) Representative immunoblot image depicting cytoplasmic and nuclear fractions of healthy controls (CT1-2 = age-matched male individuals, CT3 = age-matched female individual) and patient-derived (I#1) fibroblasts. G) Quantitated density of immunoblot bands from four independent experiments. Average values are presented as the mean \pm SEM; *** p < 0.001 significantly different from controls. In patient-derived fibroblasts, nuclear MATR3 amounts are clearly reduced.

278x158mm (150 x 150 DPI)